



Contents lists available at ScienceDirect

Bioorganic & Medicinal Chemistry Letters

journal homepage: www.elsevier.com/locate/bmcl

Substituted pyrazoles as novel sEH antagonist: Investigation of key binding interactions within the catalytic domain

Ho Yin Lo^{a,*}, Chuk C. Man^a, Roman W. Fleck^{a,†}, Neil A. Farrow^a, Richard H. Ingraham^{b,‡}, Alison Kukulka^c, John R. Proudfoot^a, Raj Betageri^a, Tom Kirrane^a, Usha Patel^a, Rajiv Sharma^a, Mary Ann Hoermann^a, Alisa Kabcenell^b, Stéphane De Lombaert^a

^aBoehringer Ingelheim Pharmaceuticals Inc., Biomolecular Screening, 900 Ridgebury Rd., PO Box 368, Ridgefield, CT 06877, USA

^bMedicinal Chemistry, Biomolecular Screening, 900 Ridgebury Rd., PO Box 368, Ridgefield, CT 06877, USA

^cCardiometabolic Diseases, Biomolecular Screening, 900 Ridgebury Rd., PO Box 368, Ridgefield, CT 06877, USA

ARTICLE INFO

Article history:

Received 2 August 2010

Revised 14 September 2010

Accepted 16 September 2010

Available online 19 September 2010

Keywords:

sEH

Pyrazoles

Aniline

EETs

Anti-hypertension

ABSTRACT

A novel series of pyrazole sEH inhibitors is reported. Lead optimization efforts to replace the aniline core are also described. In particular, 2-pyridine, 3-pyridine and pyridazine analogs are potent sEH inhibitors with favorable CYP3A4 inhibitory and microsomal stability profiles.

© 2010 Elsevier Ltd. All rights reserved.

Epoxyeicosatrienoic acids (EETs) are metabolites generated from the epoxidation of arachidonic acid by cytochrome P450 epoxygenases.¹ Four isoforms of EETs, namely the 5,6-; 8,9-; 11,12- and 14,15-EET, can be produced depending on the site of epoxidation.² They possess vasodilatory³ and anti-inflammatory properties.⁴ A number of studies have suggested that EETs are the potential endothelial derived hyperpolarizing factor (EDHF)⁵ involved in vascular, renal, and cardiac blood pressure regulation. Leveraging the beneficial physiological characteristics of EETs represents a potential new avenue for the treatment of hypertension and related end-organ damage. Towards this end, several approaches could be envisioned, including limiting EETs metabolism.

Soluble epoxide hydrolyase (Ephx2; sEH) is a cytosolic enzyme found in mammalian tissues, including liver, kidney, intestine, and the vasculature.⁶ An important enzymatic function of sEH is to hydrolyze EETs to the corresponding dihydroxyeicosatrienoic acids (DHETs).⁷ These diols are less potent vasodilators due to generally lower intrinsic activity and rapid excretion from the body. sEH serves as a major clearance mechanism for EETs and therefore is anticipated to regulate vascular homeostasis.⁸ Indeed, salt-sensi-

tive male mice deficient in the sEH-expressing gene display lower systolic blood pressure than wild type.⁹ In renal disease states derived from diabetes and hypertension, endothelial dysfunction is found to be the main cause for the condition. Inhibition of sEH may improve renal function because of increasing EETs concentration in the body.¹⁰ AUDA, prototypical sEH inhibitor, has been reported to lower mean arterial blood pressure and improve renal function in a salt-sensitive rat model.¹¹

We¹² and others^{13,14} have been interested in designing sEH inhibitors with a superior drug profile relative to AUDA and from a distinct structural class to strengthen the proof-of-concept beyond lipophilic ureas. We have previously reported benzamides^{12a,b} and more polar ureas^{12c,d} as potent sEH inhibitors. We now report on a novel structural series resulting from a focused high-throughput screening campaign. The lead compound **1**, with an IC₅₀ of 41 nM to human sEH, was readily co-crystallized with human sEH protein (Fig. 1) to gain precise information on the key binding interactions of the inhibitor with the enzyme. The X-ray structure reveals that compound **1** resides within the catalytic domain of sEH: TYR383 and TYR466 form H-bonds with the carbonyl group of the inhibitor and the catalytic ASP335, responsible for the hydrolysis of epoxide, engages an H-bond with the amide proton. This 'triple' interaction is crucial for the inhibitor to achieve high affinity, since either replacing the carbonyl or removing the amide proton (e.g., N-methylation) resulted in a substantial loss of potency (data not shown).

* Corresponding author. Tel.: +1 203 798 4923.

E-mail address: ho-yin.lo@boehringer-ingelheim.com (H.Y. Lo).

† Present address: Index Ventures.

‡ Present address: National Institutes of Health.

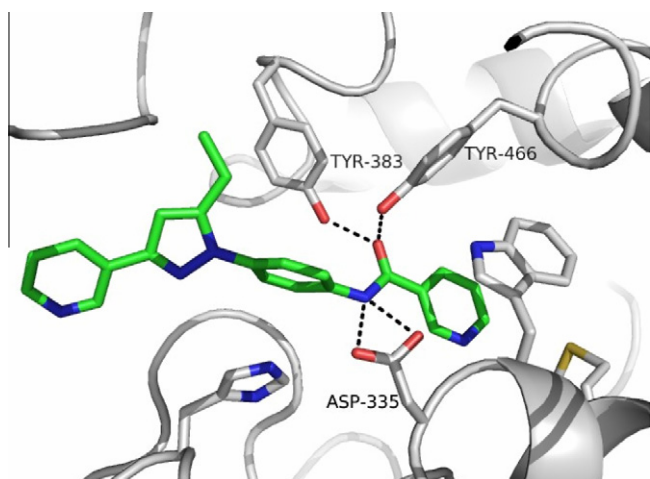


Figure 1. X-ray co-crystal structure of **1**. Coordinates of the co-crystal structure of **1** with sEH are deposited in the RCSB protein data bank (ID: rcsb061561; PDB ID: 3OTQ).

Figure 2 illustrates that both pyridine moieties are facing open channels pointing towards the solvent. The ethyl group of the inhibitor resides in a deep hydrophobic pocket of the protein.

Some conservative structural modifications of **1**, consistent with the binding model, have provided additional information to guide the lead optimization (Table 1). Replacement of the ethyl substitution in the pyrazole ring with trifluoromethyl moiety (e.g., **2**) led to a small improvement in potency. However, changing the right-hand-side (RHS) 3-pyridine to a 4-pyridine or phenyl group resulted in a threefold improvement in potency (**3**: $IC_{50} = 7.3$ nM).¹⁵

Although compound **3** showed an attractive potency level, the potential generation of an aniline moiety in the molecule by metabolic hydrolysis was considered a potential liability for drug toxicity. It is well documented that aniline and related structures link to idiosyncratic toxicity,¹⁶ mutagenesis,¹⁷ splenotoxicity¹⁸ and renal toxicity¹⁹ in different xenobiotics. The proposed mechanism for the toxicity involves N-hydroxylation and subsequent reactions with macromolecular nucleophiles (such as DNA) in vivo to generate an aniline-MN (macromolecular nucleophile) adduct (Fig. 3) and leads to adverse drug reactions as mentioned above.

First, we investigated the possibility of replacing the aniline moiety in the inhibitor while attempting to maintain the key binding interactions with the catalytic domain of sEH. The reverse

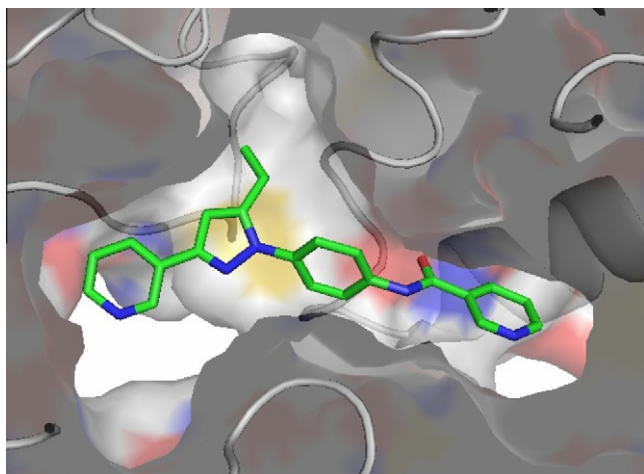


Figure 2. Surface representation of the X-ray co-crystal of sEH and **1**.

Table 1
Representative modifications

Compound	R ¹	R ²	Human sEH (IC_{50}) (nM) ^{a,b}
1	CH ₂ CH ₃	*-	41
2	CF ₃	*-	23
3	CF ₃	*-	7.3
4	CF ₃	*-	6.2

^a Values are means of a minimum of two experiments.

^b See Ref. 15 for details of the binding assay.

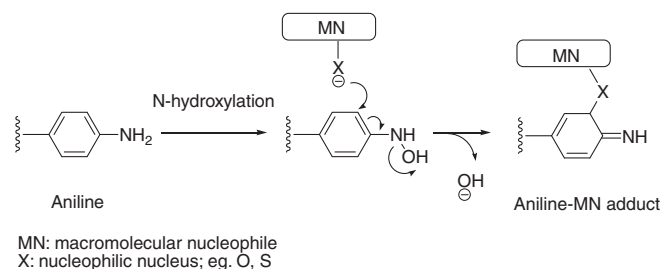
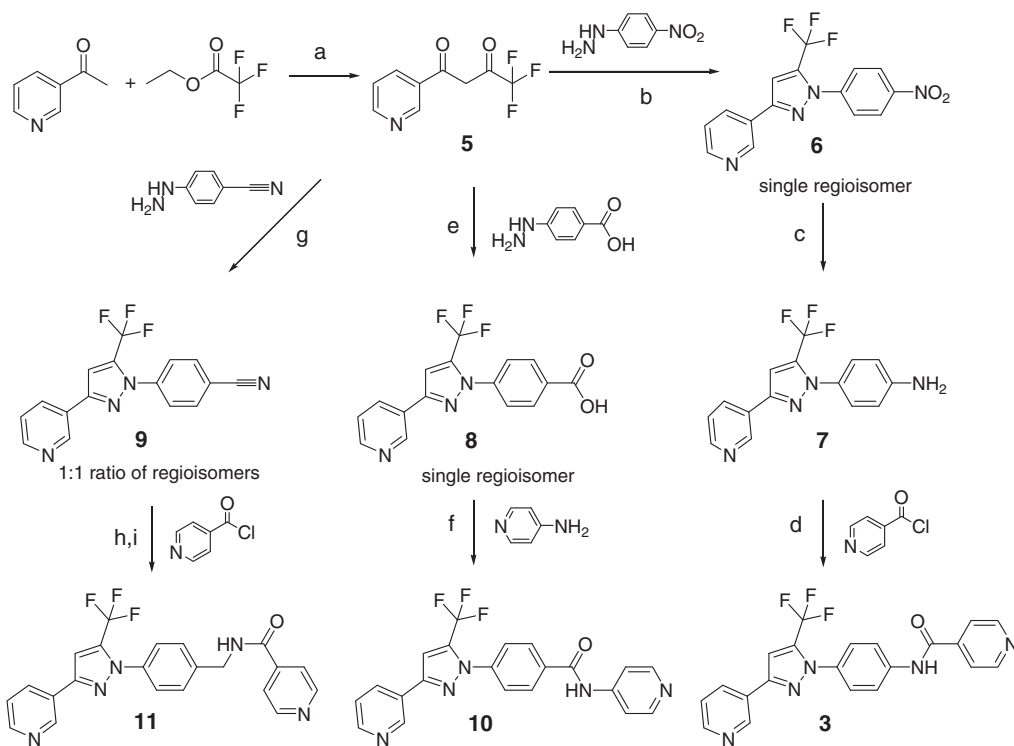


Figure 3. Oxidative alkylation of aniline related structural feature.

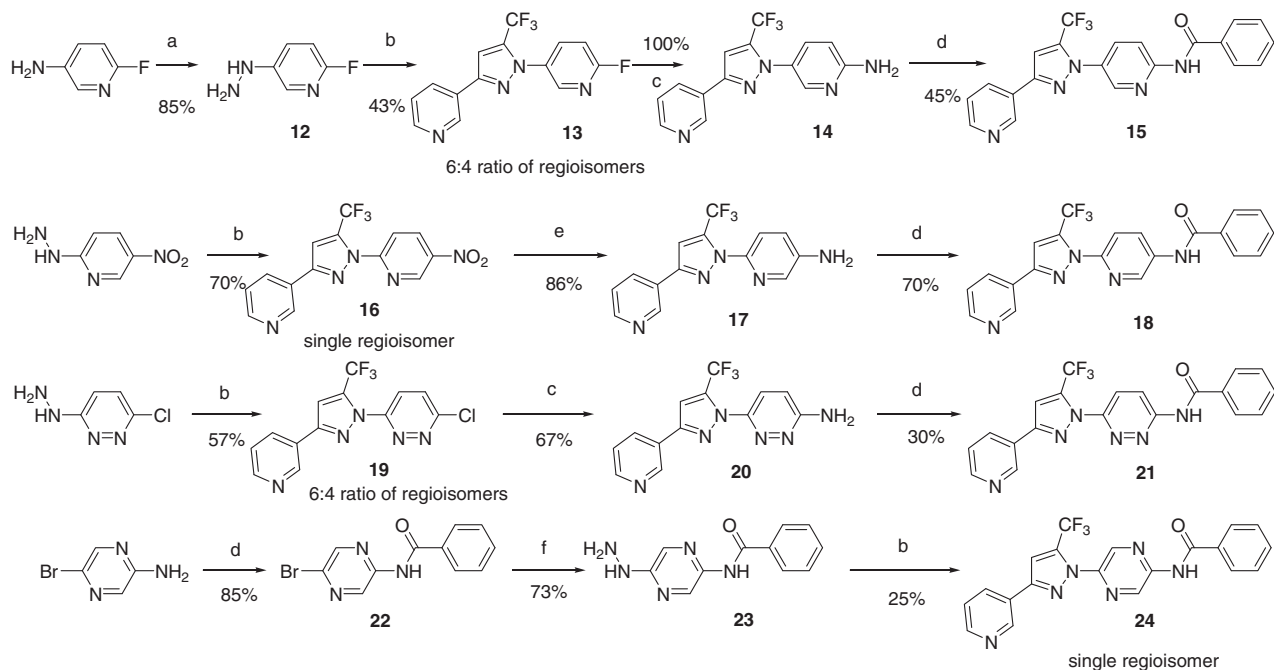
amide analog **10** and benzyl amide **11** were first considered as an aniline replacement. The syntheses of **3**, **10** and **11** started with aldol condensation of ethyl trifluoroacetate and 3-acetylpyridine to generate the 1,4-diketone building block **5** (Scheme 1). Compound **5** was then reacted with 4-cyanophenylhydrazine, 4-hydrazinobenzoic acid and 4-nitrophenylhydrazine to yield the corresponding pyrazole intermediates **9**, **8** and **7**, respectively. In the case of compounds **7** and **8**, only the desired regioisomers were obtained. However for compound **9**, a pair of chromatographically separable regioisomers was obtained in 1:1 ratio (structures assigned by NOESY experiments). Reverse amide analog **10** and benzyl amide analog **11** were obtained in moderate yields by simple functional group transformations.

To our disappointment, when compared with the lead compound **3**, the activities of compound **10** and **11** were significantly weaker (61- and 89-fold loss) (Table 2). From this result, the atomic geometry of the aniline amide structure in compound **3** was believed to be optimal for interacting with the three key residues in the catalytic domain. Therefore, instead of modifying the 'amide portion' of the molecule, our attention shifted to the 'aromatic portion' and aimed at replacing the core benzene ring with various six-membered nitrogen containing heteroaromatics, since there are reports showing that they are much less mutagenic than the aniline.²⁰ The reason behind could be the relatively low rate of enzymatic N-hydroxylation for those heteroaromatics.

The syntheses of 2-pyridine **15**, 3-pyridine **18**, pyridazine **21** and pyrazine **24** analogs are described in Scheme 2. The formation of pyrazole units in those analogs follows the procedure applied for accessing compound **3** from the corresponding hydrazine intermediates. The synthesis of pyrimidine analog **28** proved to be more challenging. As shown in Scheme 3, pyrazole intermediate **25**



Scheme 1. Synthetic route for amide, reverse amide and benzyl amine analogs. Reagents and conditions: (a) NaOMe, MeOH, reflux, 50%; (b) (i) 4-nitrophenylhydrazine, EtOH, reflux; (ii) acetic acid, 100 °C, 46%; (c) Pd/C, H₂, 1 atm., EtOH, rt, 97%; (d) isonicotinoyl chloride, Et₃N, CH₂Cl₂, 50%; (e) (i) 4-hydrazinobenzoic acid, EtOH, reflux; (ii) acetic acid, 100 °C, 25%; (f) 4-aminopyridine, 1-[3-(dimethylamino)propyl]-3-ethylcarbodiimide, rt, 32%; (g) (i) 4-cyanophenylhydrazine, EtOH, reflux; (ii) acetic acid, 100 °C, 12%; (h) LiAlH₄, Et₂O, 0 °C, 70%; (i) isonicotinoyl chloride, Et₃N, CH₂Cl₂, 27%.



Scheme 2. Synthetic route for 2-pyridine, 3-pyridine, pyridazine and pyrazine analogs. Reagents and conditions: (a) NaNO₂, SnCl₂, HCl; (b) (i) **5**, EtOH, reflux; (ii) acetic acid, 100 °C; (c) NH₃/MeOH, 150 °C; (d) benzoyl chloride, pyridine; (e) Pd/C, H₂, 1 atm., EtOH; (f) N₂H₄, EtOH, 100 °C, microwave.

was obtained as a pair of separable regioisomers by condensation reaction of **5** with ethyl hydrazinoacetate. The desired regioisomer **25** was then hydrolyzed and reacted with DMF under POCl₃ and NaPF₆ condition to generate the corresponding vinamidinium salt **26**.²¹ The pyrimidine core **27** was formed by a condensation

reaction of **26** with guanidine carbonate. The target compound **28** was obtained by an acylation reaction of **27** with benzoyl chloride.

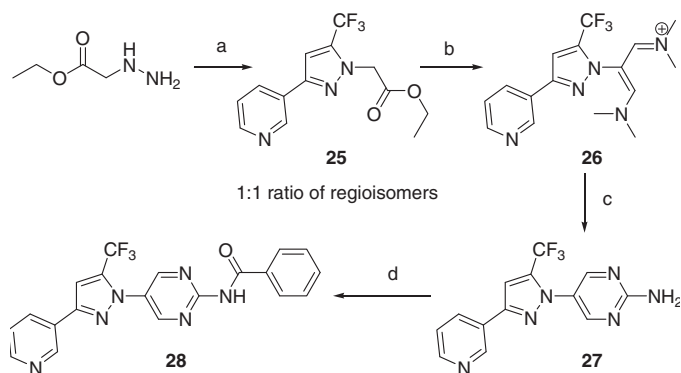
The biological activities of these heterocycles are summarized in Table 3. The binding affinities of the 2-pyridine **15**, 3-pyridine

Table 2
Modification of amide

Compound	Human sEH (IC ₅₀) (nM) ^{a,b}
3	7.3
10	450
11	650

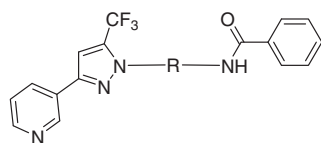
^a Values are means of a minimum of two experiments.

^b See Ref. 15 for details of the binding assay.



Scheme 3. Synthetic route for pyrimidine analog. Reagents and conditions: (a) **5**, HCl, EtOH, 80 °C, 58%; (b) (i) LiOH, MeOH; (ii) POCl₃, NaPF₆, DMF, 52%; (c) NaH, guanidine carbonate, EtOH, 80 °C, 48%; (d) benzoyl chloride, iPr₂NEt, 48%.

Table 3
Modification of central aromatic ring



Compound	R	Human sEH (IC ₅₀) (nM) ^{a,b}
4		6.2
15		4.7
18		9.9
21		8.8
24		28
28		21

^a Values are means of a minimum of two experiments.

^b See Ref. 15 for details of the binding assay.

Table 4
Profiles of representative compounds

Compound	Human sEH (IC ₅₀) (nM) ^{a,b}	Human sEH DPPO (IC ₅₀) (nM) ^{a,c}	CYP3A4 (IC ₅₀) (μM) ^a	h-LM (%Qh) ^a
4	6.2	1	NT ^d	NT ^d
15	4.7	5	>30	36
18	9.9	397	NT ^d	NT ^d
21	8.8	83	>30	31

^a Values are means of a minimum of two experiments.

^b See Ref. 15 for details of the binding assay.

^c See Ref. 22 for details of the cell assay.

^d NT: not tested.

18, and pyridazine **21** to sEH are equivalent to aniline analog **4**. The positive results from this modification indicated that alterations of the electronic property of the central aromatic core had minimal impact on the binding activity.

However, there was a slight drop in potencies for pyrazine analog **24** and pyrimidine analog **28**. The reason for the loss of binding activity is not fully understood at this point. It could be speculated that there might be a subtle alteration of the torsional angle between the left hand side pyrazole and the core aromatic system in analog **24** and **28**, which leads to less favorable binding and results in lost of potencies.

The encouraging binding potencies of compounds **15**, **18** and **21** prompted us to further profile them in various in vitro assays (Table 4). In a human sEH DPPO cellular assay,²² 2-pyridine analog **15** showed superior activity over 3-pyridine **18** and pyridazine **21**. The deep drop in cell activity of **18** might result from its inferior cell permeability (consistent with its very poor caco-2 result). Both **15** and **21** have good selectivity over CYP3A4 (>30 μM) and moderate human liver microsomal stabilities (36% and 31%, respectively). Overall, 2-pyridine analog **15** processes a very attractive profile for further lead optimization.

In conclusion, we have discovered a novel series of small molecules sEH inhibitors featuring pyrazole and aniline structural moieties. Successful replacement of the aniline with 2-pyridine, 3-pyridine or pyridazine rings maintains high inhibitory potency and favorable CYP3A4 inhibitory and microsomal stability profiles. The optimization of this pyrazole series toward potential drug candidates and their pharmacological characterization will be reported in due course.

References and notes

- Roman, R. J. *Physiol. Rev.* **2002**, *82*, 131.
- Zeldin, D. C. *J. Biol. Chem.* **2001**, *276*, 36059.
- (a) Watanabe, H.; Vriens, J.; Prenen, J.; Droogmans, G.; Voets, T.; Nilius, B. *Nature* **2003**, *424*, 434; (b) Earley, S.; Heppner, T. J.; Nelson, M. T.; Brayden, J. E. *Circ. Res.* **2005**, *97*, 1270.
- (a) Liu, Y.; Zhang, Y.; Schmelzer, K.; Lee, T.; Fang, X.; Zhu, Y.; Spector, A. A.; Gill, S.; Morisseau, C.; Hammock, B. D.; Shyy, J. Y. *Proc. Natl. Acad. Sci. U.S.A.* **2005**, *102*, 16747; (b) Node, K.; Huo, Y.; Ruan, X.; Yang, B.; Spiecker, M.; Ley, K.; Zeldin, D. C.; Liao, J. K. *Science* **1999**, *285*, 1276; (c) Kozak, W.; Kluger, M. J.; Kozak, A.; Wachulec, M.; Dokladny, K. *Am. J. Physiol.* **2000**, *279*, R455.
- Spector, A. A.; Fang, X.; Snyder, G. D.; Weintraub, N. L. *Prog. Lipid Res.* **2004**, *55*.
- (a) Wang, P.; Meijer, J.; Guengerich, F. P. *Biochemistry* **1982**, *21*, 5769; (b) Yu, Z.; Davis, B. B.; Morisseau, C.; Hammock, B. D.; Olson, J. L.; Kroetz, D. L.; Weiss, R. H. *Am. J. Physiol.* **2004**, *286*, F720.
- Hopmann, K. H.; Himo, F. *Chem. Eur. J.* **2006**, *12*, 6898.
- (a) VanRollins, M.; Kaduce, T. L.; Knapp, H. R.; Spector, A. A. *J. Lipid Res.* **1993**, *34*, 1931; (b) Weintraub, N. L.; Fang, X.; Kaduce, T. L.; VanRollins, M.; Chatterjee, P.; Spector, A. A. *Am. J. Physiol.* **1999**, *277*, H2098.
- Sinal, C. J.; Miyata, M.; Tohkin, M.; Nagata, K.; Bend, J. R.; Gonzalez, F. J. *J. Biol. Chem.* **2000**, *275*, 40504.
- Imig, J. D. *Am. J. Physiol. Renal. Physiol.* **2005**, *289*, F496.
- Imig, J. D.; Zhao, X.; Zaharis, C. Z.; Olearczyk, J. J.; Pollock, D. M.; Newman, J. W.; Kim, I.; Watanabe, T.; Hammock, B. D. *Hypertension* **2005**, *46*, 975.
- (a) Eldrup, A. B.; Soleymanzadeh, F.; Taylor, S. J.; Muegge, I.; Farrow, N. A.; Joseph, D.; McKellop, K.; Man, C. C.; Kukulka, A.; De Lombaert, S. *J. Med. Chem.* **2009**, *52*, 5880; (b) Taylor, S. J.; Soleymanzadeh, F.; Eldrup, A. B.; Farrow, N. A.; Muegge, I.; Kukulka, A.; Kabcenell, A. K.; De Lombaert, S. *Bioorg. Med. Chem. Lett.* **2009**, *19*, 5864; (c) Eldrup, A. B.; Soleymanzadeh, F.; Farrow, N. A.; Kukulka, A.; De Lombaert, S. *Bioorg. Med. Chem. Lett.* **2010**, *20*, 571; (d) Kowalski, J. A.; Swinamer, A. D.; Muegge, I.; Eldrup, A. B.; Kukulka, A.; Cywin, C. L.; De Lombaert, S. *Bioorg. Med. Chem. Lett.* **2010**, *20*, 3703.
- Representative publications from Arête Therapeutics and University of California, Davis: (a) Anandan, S.-K.; Gless, R. D. *Bioorg. Med. Chem. Lett.* **2010**, *20*, 2740; (b) Anandan, S.-K.; Webb, H. K.; Do, Z. N.; Gless, R. D. *Bioorg. Med. Chem. Lett.* **2009**, *19*, 4259; (c) Anandan, S.-K.; Do, Z. N.; Webb, H. K.; Patel, D. V.; Gless, R. D. *Bioorg. Med. Chem. Lett.* **2009**, *19*, 1066; (d) Kasagomi, T.; Kim, I.-H.; Tsai, H.-J.; Nishi, K.; Hammock, B. D.; Morisseau, C. *Bioorg. Med. Chem. Lett.* **2009**, *19*, 1784; (e) Hwang, S. H.; Tsai, H.-J.; Liu, J.-Y.; Morisseau, C.; Hammock, B. D. *J. Med. Chem.* **2007**, *50*, 3825; (f) Kim, I.-H.; Morisseau, C.; Watanabe, T.; Hammock, B. D. *J. Med. Chem.* **2004**, *47*, 2110.
- Representative publications from Merck: (a) Shen, H. C.; Ding, F.-X.; Wang, S.; Deng, Q.; Zhang, X.; Chen, Y.; Zhou, G.; Xu, S.; Chen, H.-S.; Tong, X.; Tong, V.; Mitra, K.; Kumar, S.; Tsai, C.; Stevenson, A. S.; Pai, L.-Y.; Alonso-Galicia, M.; Chen, X.; Soisson, S. M.; Roy, S.; Zhang, B.; Tata, J. R.; Berger, J. P.; Colletti, S. L. *J. Med.*

- Chem.* **2009**, *52*, 5009; (b) Shen, H. C.; Ding, F.-X.; Wang, S.; Xu, S.; Chen, H.-S.; Tong, X.; Tong, V.; Mitra, K.; Kumar, S.; Zhang, X.; Chen, Y.; Zhou, G.; Pai, L.-Y.; Alonso-Galicia, M.; Chen, X.; Zhang, B.; Tata, J. R.; Berger, J. P.; Colletti, S. L. *Bioorg. Med. Chem. Lett.* **2009**, *19*, 3398; (c) Shen, H. C.; Ding, F.-X.; Deng, Q.; Xu, S.; Chen, H.-S.; Tong, X.; Tong, V.; Zhang, X.; Chen, Y.; Zhou, G.; Pai, L.-Y.; Alonso-Galicia, M.; Zhang, B.; Roy, S.; Tata, J. R.; Berger, J. P.; Colletti, S. L. *Bioorg. Med. Chem. Lett.* **2009**, *19*, 5314; (d) Shen, H. C.; Ding, F.-X.; Deng, Q.; Xu, S.; Tong, X.; Zhang, X.; Chen, Y.; Zhou, G.; Pai, L.-Y.; Alonso-Galicia, M.; Roy, S.; Zhang, B.; Tata, J. R.; Berger, J. P.; Colletti, S. L. *Bioorg. Med. Chem. Lett.* **2009**, *9*, 5716.
15. Details for the binding assay: Test compounds were dissolved and serially diluted in DMSO, with final dilution in assay buffer (20 mM TES, 200 mM NaCl, 0.05% w/v CHAPS, 1 mM TCEP, pH 7.0) to achieve 1% DMSO in the assay. Test compounds were dispensed into a black, flat-bottom 96-well plate. Positive controls were reaction mixtures containing no test compound; negative controls (blanks) were reaction mixtures containing a reference inhibitor. The reaction was started with the addition of a mixture of either human or rat SEH (final assay concentration is 10 nM) and probe (final assay concentration is 2.5 nM). The reaction was mixed by briefly shaking the plate on an orbital shaker, and the plates were incubated in the dark for 30 min at room temperature. Fluorescence polarization is measured on an LJL Analyst using a 530 nm excitation filter, a 580 nm emission filter, and a 561 nm dichroic mirror. Concentration–response data were fitted to a 4-parameter equation to determine IC₅₀ values. Also see US2003/0082665.
16. Mitchell, J. R.; Jollow, D. J.; Potter, W. Z.; Gillette, J. R.; Brodie, B. B. *J. Pharmacol. Exp. Ther.* **1973**, *187*, 211.
17. (a) Lin, J.-K.; Miller, J. A.; Miller, E. C. *Cancer Res.* **1975**, *35*, 844; (b) Chung, K.-T.; Murdock, C. A.; Zhou, Y., Jr.; Edward Stevens, S.; Li, Y.-S.; Wei, C.-I.; Fernando, S. Y.; Chou, M.-W. *Environ. Mol. Mutagen.* **1996**, *27*, 67.
18. (a) Khan, M. F.; Wu, X.; Kaphalia, B. S.; Boor, P. J.; Ansari, G. A. S. *Toxicology* **2003**, *194*, 95; (b) Wang, J.; Kannan, S.; Li, H.; Khan, M. F. *Toxicol. Appl. Pharm.* **2005**, *203*, 36.
19. Hong, S. K.; Anestis, D. K.; Henderson, T. T.; Rankin, G. O. *Toxicol. Lett.* **2000**, *114*, 125.
20. (a) Ho, C.-H.; Clark, B. R.; Guerin, M. R.; Barkenbus, B. D.; Rao, T. K.; Epler, J. L. *Mutat. Res.* **1981**, *85*, 335; (b) Wakabayashi, K.; Yahagi, T.; Nagao, M.; Sugimura, T. *Mutat. Res.* **1982**, *105*, 205; (c) Borosky, G. L. *Chem. Res. Toxicol.* **2007**, *20*, 171.
21. Gupton, J. T.; Hicks, F. A.; Smith, S. Q.; Main, A. D.; Petrich, S. A.; Wilkinson, D. R.; Sikorski, J. A.; Katritzky, A. R. *Tetrahedron* **1993**, *49*, 10205.
22. Borhan, B.; Mebrahtu, T.; Nazarian, S.; Kurth, M. J.; Hammock, B. D. *Anal. Biochem.* **1995**, *231*, 188.